# **Book Chapter**

# Non-Contact Real-Time Detection and Monitoring of Microbial Contaminants on Solid Surfaces Using Medium- (BC-Sense) and Short-Distance (H2B-Spectral) Range Sensors

O Rebane<sup>1</sup>, S Babichenko<sup>1</sup>, M Bentahir<sup>2</sup>, L Poryvkina<sup>1</sup> and JL Gala<sup>2</sup>\*

<sup>1</sup>LDI Innovation OÜ, 7 Sära tee, Peetri 75312, Estonia <sup>2</sup>Center for Applied Molecular Technologies, Institute of Clinical and Experimental Research, Université catholique de Louvain, Belgium

\*Corresponding Author: JL Gala, Center for Applied Molecular Technologies, Institute of Clinical and Experimental Research, Université catholique de Louvain, Tour Claude Bernard, Avenue Hippocrate 54-55, B1.54.01, 1200 Brussels, Belgium

#### Published December 20, 2021

How to cite this book chapter: O Rebane, S Babichenko, M Bentahir, L Poryvkina, JL Gala. Non-Contact Real-Time Detection and Monitoring of Microbial Contaminants on Solid Surfaces Using Medium- (BC-Sense) and Short-Distance (H2B-Spectral) Range Sensors. In: Prime Archives in Public Health. Hyderabad, India: Vide Leaf. 2021.

© The Author(s) 2021. This article is distributed under the terms of the Creative Commons Attribution 4.0 International License (http://creativecommons.org/licenses/by/4.0/), which permits unrestricted use, distribution, and reproduction in any medium, provided the original work is properly cited.

**Acknowledgement:** This work has received funding from the European Union Seventh Framework Programme (FP7/2007-2013), theme security (SEC), FP7-SEC EDEN project (End-user driven Demo for cbrNe) under the Grant no. 313077, H2020 project eNOTICE (European Network of CBRN Training Centres) under Grant Agreement No. 740521 (https://www.h2020-enotice.eu/, accessed on 18 August 2021), and ERDF project EU53450 (H2B-Spectral - development of a hand-held biocontamination detector).

#### **Abstract**

Real-time detection and monitoring (RTDM) of microbial contamination on solid surfaces is mandatory in a range of security, safety, and biomedical applications where surfaces are exposed to natural. accidental or intentional microbial contamination. This work presents the RTDM results obtained with two new devices, i.e. the BC-Sense and the H2B-Spectral sensors. Both tools allow a rapid and user-friendly RTDM of microbial contamination on various surfaces while assessing the decontamination kinetics and degree of cleanliness. The BC-Sense is a stand-off LIDAR (Light Detection And Ranging) device using the Light-Induced Fluorescence (LIF) method based on dual-wavelength sensing with a multispectral pattern recognition system to rapidly detect and classify microbial contamination on a solid surface at medium-distance range. In contrast, the H2B-Spectral is a compact sensor using the LIF method with dual-wavelength sensing in non-contact mode at short distances. Both devices allow real-time control of the contamination before. during, and surface decontamination procedure. Accordingly, their performance was evaluated in operator-induced contamination experiments, using microbial simulants (bacteria, bacterial spores, fungal conidia, and viruses) spread on various solid surfaces. The limit of detection (LoD) of E. coli and MS2 virus were 2.9 x10<sup>4</sup> and 9.5 x 10<sup>4</sup> PFU and CFU/cm<sup>2</sup>, respectively. The LoD of bacteria detection with H2B-Spectral was as little as 2 x 10<sup>3</sup> CFU/cm<sup>2</sup>. Random samples (n=200) tested against a training dataset (n=800) were optimally discriminated for contamination versus background with a threshold of predicted response (PR) > 0.55

and < 0.4, respectively with BC-Sense. The kinetics of decontamination by vaporized hydrogen peroxide (VHP) of the spores of *Bacillus atrophaeus* (BA) measured with the H2B-Spectral device revealed the bi-exponential fluorescence quenching function of the fluorescence intensity and the VHP decontamination agent concentration, backed with a model of underlying processes. This paper provides evidence of the validity of the LIF method realised in the stand-off and noncontact modes and its feasibility for the RTDM application for medium- (BC-Sense) and short-distance (H2B-Spectral) ranges.

#### Introduction

The common thread of microbial contamination is the exposition of solid surfaces to the accidental, natural, or intentional deposit of micrometer- and submicrometer-sized particles consisting of contaminating biological agents, loosely defined as microbial contaminants. In many cases, the need for assessing readily and rapidly the materiality and extent of biological contamination is of paramount importance [1]. This commonly applies to incidents where an accidental, natural, or deliberate release of microbial contaminants is suspected. Scenarios, where real-time monitoring (RTDM) is detection and mandatory, synthetically be split in a preventive versus reactive approach. The preventive approach applies to many situations, e.g. to microbiological analyses of surfaces in the food-processing industry where RTDM is part of the tools used to control the hygiene of food products, to the microbial control of industrial and hospital clean-room facilities, to the control of cleanliness in operating theatres, and as a biosafety measure in microbiological or medical laboratories. The reactive approach occurs after the suspicion of a deliberate or accidental release of biological agents. It is used to assess the extent of surface contamination, delineate as precisely as possible the area to be excluded for nonauthorized persons, and guide the sampling procedures while avoiding unnecessary random sampling. Assessment of the decontamination efficiency, which is commonly quoted as "how clean is clean enough", takes place after the cleaning phase following the dispersion of biological aerosol [2]. Whether in civilian, public health, or military context, it undoubtedly remains a key issue.

Conventional methods require the samples to be taken in the 'right spot' to accurately assess the presence and/or distribution of the microbial flora. It is however impossible to sample large areas/volumes or continuously sample with current technology. Due to biosafety issues, sample contact itself is a major concern in most situations. Technologies capable of providing a noncontact, real-time detection of microbiological contaminants and real-time assessment during and after decontamination are extremely scarce. Thev include fluorescence (photoluminescence) spectroscopy [3,4], Raman spectroscopy [5], Laser-Induced Breakdown Spectroscopy (LIBS) [6], and hyperspectral imaging [7]. Each of these techniques has its merits and drawbacks. Compared with fluorescence, the Raman spectroscopy would need at least one order of magnitude more power than fluorescence and a much more stable wavelength to generate a signal-to-noise ratio that is exploitable irrespective of the absence of the fluorescence background known to be a hindrance. LIBS spectroscopy would need several orders of magnitude more power per pulse and a higher-resolution and lower throughput spectrometer while the hyperspectral imaging system might not be specific enough and needs controlling ambient light. The auto fluorescence's high sensitivity and selectivity are therefore considered to be suitable and effective features to use in the RTDM of small amounts of microbial contaminants on surfaces at medium-range distances. The intrinsic fluorescence of various biomolecules depends not only on the concentration of fluorescing molecules (e.g. tryptophan) contained in the proteins of biological agents, but also depends on the molecular composition of the immediate surroundings (i.e. the chemical background/solvent). This can cause large changes in registered spectra due to the energy transfer [8] or quenching of the emitted fluorescence spectrum. Consequently, the shape of the induced fluorescence spectrum reflects specifically the molecular composition of the assessed area, hence can serve for detection and monitoring of various microbiological agents.

This book chapter describes the development of the sensors using the Light Induced Fluorescence (LIF) method for RTDM applications on solid surfaces. A medium- and short-distance

range applications are reported, i.e. the BC-Sense (Figure 1a) and H2B-Spectral (Figure 1b) sensors. The stand-off BC-Sense LIDAR system is based on dual-wavelength laser remote sensing with multispectral pattern recognition and is dedicated to remote detection (up to 20 m) of microbiological agents on solid surfaces in the indoor environment. The non-contact H2B-Spectral sensor is used as point detector for short-distance (few centimeters) range applications. The working mechanism of this hand-held point detector is based on dual-wavelength sensing of surface contamination, using UV-LEDs and SiPM spectral detectors. To assess the performance of both devices for RTDM of microbial contamination, we used a panel of biological agents spread on various solid materials as a model of natural, accidental or intentional contaminations. The performance of the H2B-Spectral sensor was evaluated using vaporized hydrogen peroxide (VHP)-based real-time decontamination in experiments.



Figure 1: Pictures of BC-Sense (a) and H2B-Spectral (b) sensors

Materials and Methods

Description of the BC-Sense Device

The BC-Sense LIDAR system was developed for stand-off detection of microbial agents on the materials and surfaces. The working range of the device is from 5 to ~20 m, which is defined as a medium-distance range suitable for indoor microbial assessment, for instance the inspection of poorly accessible construction and infrastructure elements (e.g. walls, ventilation

systems, working surfaces). It consists of 2 excimer lasers that induce the fluorescence, a telescope to collect the backscattered fluorescence signal, a spectrometer with switchable long-pass filters, an intensified linear light detector for detecting low-level signals, and other components including the electronic controller (Figure 1a).

Fluorescence from the sample is excited by a 248 nm krypton fluoride (KrF) and 351 nm xenon fluoride (XeF) laser with ~5 and ~2 mJ pulse energy, respectively (Figure 2). The lasers operated with the pulse repetition rate of 10 Hz. The optical scheme of the LIDAR is co-axial, which means that the laser beam and the telescope are always aligned along the optical axis of the device. This means that changing the distance between the sensor and the surface to assess does not require adjusting the basic optical setup of the LIDAR nor to have moving parts when the focus distance ranges from 5 to 20 m. Moreover, the reflective-only optical scheme means that chromatic aberrations or spectral shifts with distance are unlikely. The co-axial and achromatic alignment allows for continuous measurement without requiring constant adjustments by the operator or the software.

The laser light is directed onto the target surface in trains/sequences of consecutive pulses (10 pulses at both wavelengths by default). The backscattered light, containing scattering and fluorescence flux, is collected by an off-axis parabolic mirror telescope, and the reflected (same-wavelength) laser light is removed before entering the spectrometer by switchable long pass filters. The fluorescence at each excitation wavelength is dispersed into a spectrum with a concave diffraction grating. The spectrum is recorded by the intensified time-gated multi-channel linear detector. It allows the system to be operated by users in daylight conditions. The spectral resolution is about 10 nm in the wavelength range from 300 nm to 600 nm. The microcontroller manages the operational cycle of the system and sends the data package for storage and analysis.

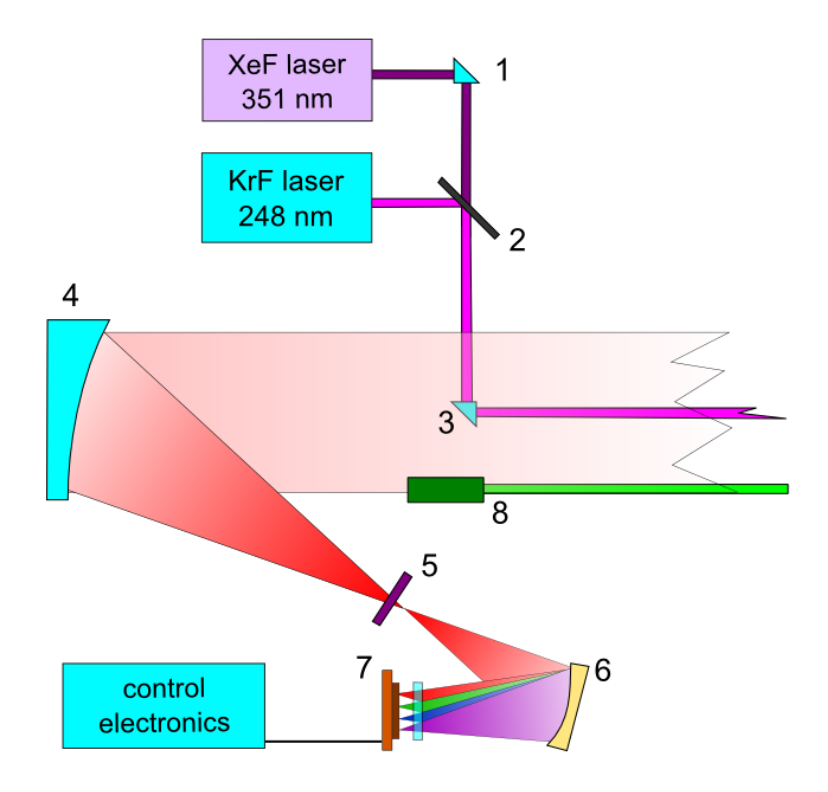


**Figure 2:** The operational scheme of BC-Sense device. Prisms (1, 3), dichroic filter (2) - telescope mirror, switchable laser-line cut-off filter (5), diffraction grating 6), gated and amplified linear light detector (7), laser pointer (8).

The BC-Sense device can be carried by two persons and operated on a special trolley (Figure 1a). The dimensions of the LIDAR device are 680 x 410 x 337 mm and it weighs 40 kg. A special trolley was created to allow for easily directing and aiming the laser beam from the LIDAR onto the target. A green laser pointer was installed into the LIDAR to help aim target areas. The power consumption of the air-cooled and wall-plug-powered device is 200 W. With respect to both excitation wavelengths, the 248 nm wavelength induces the fluorescence of protein residues contained in all microorganisms, namely tryptophan, tyrosine, and phenylalanine amino acids, and resulted in the emission of fluorescence around 350 nm [9]. The excitation at 351 nm induces the fluorescence of a reduced form of nicotinamide adenine dinucleotide (NADH), which is a

7

coenzyme having major metabolic functions in bacterial and fungal cells but not in viruses, and of its phosphate form (NADPH), with an emission around 450 nm [10].

A direct optical path (i.e. without mirrors) was used to detect the panel of biological contaminants in their respective media. For each assay, the sample was placed on top of a horizontal copper surface, a material devoid of background fluorescence. Positioned at a distance of about 6 m, the laser beam was then pointed at the area of the copper surface contaminated with the biological sample and the laser-induced fluorescence spectra were measured and recorded for later analysis. For each sample, an average spectrum was recorded over 10 laser shots to increase the signal-to-noise ratio.

### **Description of the H2B-Spectral Sensor**

The hand-held bio-detector H2B-Spectral is a lightweight handheld fluorometric sensor for bio-detection (Figure 1b). It is developed to detect and identify surface areas with microbial contamination in various environments and be used as monitoring tool when of bio-contamination of equipment and facilities is suspected. The sensor detects the contamination through the optical window in non-contact mode, at a distance of approximately 5 cm from the target surface. The device synchronously excites the sample with the UV-LED radiation at 280nm and 340 nm, then analyses the induced fluorescence signals, and subtracts automatically the background light in the room during each measurement (Figure 3). At 280 nm wavelength, tryptophan and tyrosine residues are excited and contribute both to intrinsic protein fluorescence whereas NADPH and NADH-like fluorescence are excited at 340 nm. The emission detection is carried out through spectral selection with high-quality OD6 optical bandpass filters at ~340nm and 460nm for tryptophan and NADPH-like fluorescence, respectively. The detection of low-level fluorescent light signal achieved using temperature-compensated silicon a photomultiplier (SiPM) detector.

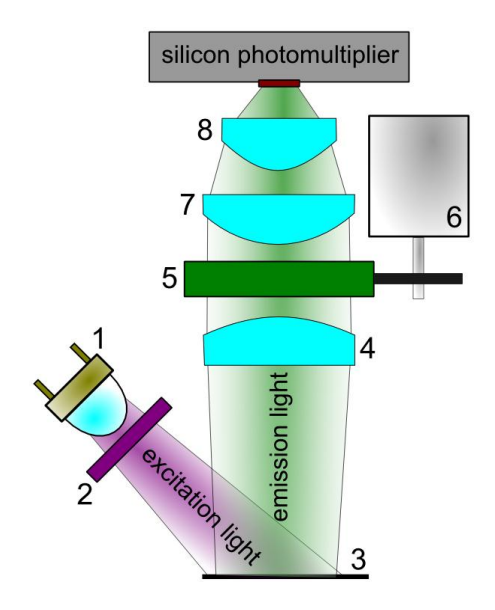


**Figure 3:** Operational scheme of H2B-Spectral sensor. Excitation LEDs (1), excitation and emission filter (2,5), sample (3), lenses for collimating and focussing the fluorescence light (4, 7, 8), filter change motor (6)

The sensor is wireless, containing a battery which provides power autonomy for several hours. Acquired data are transferred in real-time to a computer via an integrated WiFi module. In current experiments, the H2B-Spectral sensor was modified to operate continuously in RTDM mode and to measure the fluorescence intensity of the biological layer deposited on a stainless-steel plate (sample disk). The device enables to monitor the strength of the fluorescence signal during a decontamination process using vaporized hydrogen peroxide (VHP) as surface decontaminant. For this purpose, the sample compartment was designed to allow the introduction of interchangeable sample disks in the sensor, and provide controlled exposition to VHP /airflow with an integrated mini-fan.

### **Selection of a Set of Representative Solid Surfaces**

A panel of surface materials frequently exposed to biological contamination in real-life incidents or situations were selected for use during the contamination and decontamination assessment, i.e., laboratory coat, wood, Plexiglas/PMMA (poly(methyl methacrylate)), glass, galvanized steel, aluminium, rigid PVC and a UV-resistant PVC fabric (Figure 4a). The latter is a piece of the canvas tent from the B-LiFE deployable laboratory of CTMA-UCL [11-13]. Each material was cut to have a rectangular shape of 8 cm wide and 11 cm long. BC-Sense testing was carried out on the surface of the material placed on the top of the copper surface. The intrinsic fluorescence from each type of surface was assessed before spreading the biological agents (i.e. bacteria, spores, fungal conidia, and virus) (Figure 4b).

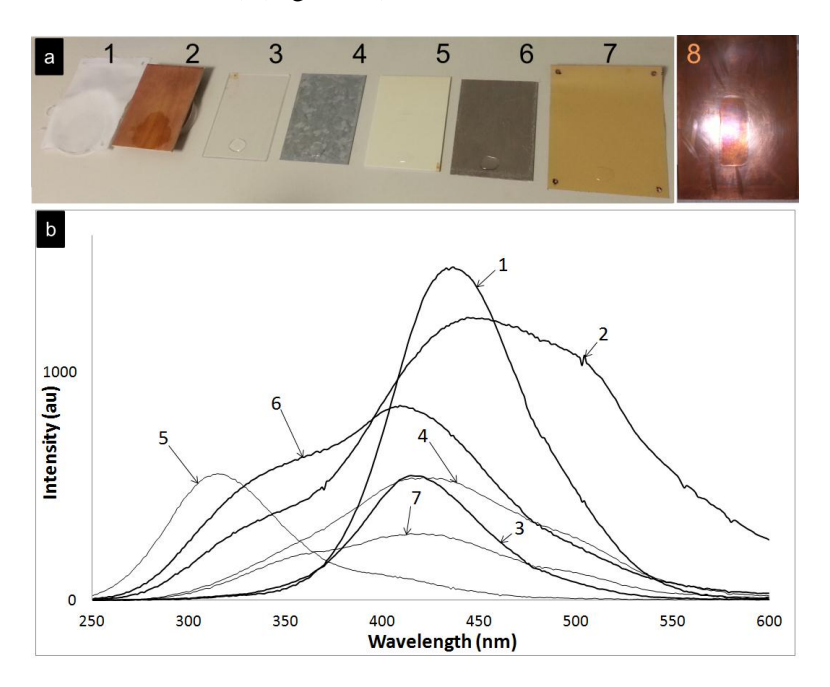


**Figure 4:** Background fluorescence of solid surfaces. Set of representative solid surfaces used for microbial contamination (a): Cloth of lab coat (1), wood (2), Plexiglas/PMMA (poly(methyl methacrylate)) (3), galvanized steel (4), PVC plastic (5), aluminium (6), canvas tent (7), copper plate (8). Corresponding gain-normalized LIF spectra of solid surfaces at the excitation 248 nm (b): spectrum of white lab coat (1) is divided by 100; the spectrum of PVC (5) is divided by 10; copper plate (8) provided no fluorescence

# Selection and Production of Biological Agents for Stand-off Detection

For this study, bacterial, bacterial spores, fungal conidia, and viral models were used as surface contaminants. E. coli, a gramnegative bacteria, is a widely used bacterial model in laboratory studies [14]. In the current study, the E. coli DSM 11250 strain (Deutsche Sammlung von Mikroorganismen und Zellkulturen, Germany) was used. B. thuringiensis, a gram-positive spore forming bacteria, is the second most studied bacteria [15] and is often used as a model, especially in decontamination studies as a surrogate for its close-neighbour Bacillus anthracis, which is a bio-warfare agent [16]. The B. thuringiensis subsp. aizawai strain ABTS-1857 was grown from Xentari WG, a commercial B. thuringiensis-based insecticide (Bayer CropScience SA-NV, Belgium). Both E. coli and B. thuringiensis strains were plated on LB agar (LB broth - VWR chemicals, Belgium; Bacto<sup>TM</sup> Agar - Becton, Dickinson and company, France) petri dish and grown overnight at 37 °C. A single colony was then transferred to a LB broth and grown overnight (37 °C, 140 rpm). The CFU/mL was determined as  $3.7 \times 10^9$  CFU/mL for E. coli and  $7.9 \times 10^7$ CFU/mL for B. thuringiensis. To prevent a high background noise due to the culture media (LB) content in tryptone and yeast extract, all biological samples used for BC-Sense measurements were resuspended and diluted in an isotonic phosphate-buffered saline (PBS). E. coli and B. thuringiensis agents were washed, resuspended in PBS buffer, and heat-inactivated (Julabo Sw22 water bath - 99°C, 80 rpm, for 3 hours) to produce a suspension of bacteria.

Spores from the *B. thuringiensis* subsp. *aizawai* strain ABTS-1857 was retrieved from the same insecticide as cited above (Xentari WG, Bayer CropScience SA-NV, Belgium). For each experiment, a fresh suspension of the Xentari powder was diluted and spiked on the surfaces, immediately before the reading.

The genus *Cladosporium*, found worldwide, is the most common outdoor and indoor environmental fungus. Different species, particularly *Cladosporium herbarum*, produce very high

concentrations of airborne conidia (asexually produced spores) responsible of respiratory allergies [17]. The strain *C. herbarum CTMA/189*, which was isolated from the air in Belgium in 2008, was grown for 8 days on agar slant (modified Sabouraud medium) to obtain an abundant production of aerial conidia. Tris-buffered saline (TBS) solution with 2 drops of Tween 80 was added to the slant, and conidia were liberated into the liquid by scrapping the surface of the colony. The conidia suspension was pipetted and placed inside a 15 mL Falcon tube (stock solution).

The bacteriophage MS2, a small-sized icosahedral RNA virus commonly used as a simulant for pathogenic viruses in a large number of studies [18], was produced as previously described by Bentahir M, *et al.* [19]. The MS2 viral titre of the cell lysate was determined by the culture method using the double agar overlay phage assay (DAL) [20]. The MS2 stock solution is at 1.24 x 10<sup>10</sup> PFU/mL.

# **Testing for Surface Contamination**

Each bacterial, viral or fungal sample was diluted to a predefined concentration. The liquid sample containing the biological contaminant (10 ml) was spread on an 8 x 11 cm area of the horizontal copper surface to form a wet area of ~100 cm² as the target surface hit by the laser beam. The reading was carried out as described above under paragraph "Principles of use of the BC-Sense device". While LIDAR measurements were all carried out with biological agent suspensions, replicated measurements on dried contaminated surfaces (i.e., surfaces let to dry after deposition of the microbial contaminated solution) did not change the recorded spectrum. Considering the time for surfaces to dry and the number of experiments, it was therefore decided for very practical reasons to pursue the work on wet surfaces and to carry out the measurements shortly after spreading a sample on a surface.

The linearity of the measures was tested by a serial dilution of *E. coli* and MS2 bacteriophage in a water-based solution. Data were used to construct a calibration curve in order to accurately calculate the limits of detection (LoD) and quantification (LoQ)

of both agents. The LoQ, which is set at a higher concentration than the LoD, is the lowest concentration at which the analyte can not only be reliably detected but at which some predefined goals for bias and imprecision are met [21]. LoD and LoQ are two important values for assessing sensitivity and performance characteristics in a validation trial.

Different concentrations (n=5) and several replicates measurements (n=4) were used for building the calibration curve. Samples were prepared by diluting the stock solution of living *E. coli* and MS2 bacteriophage virus by tenfold serial dilutions to find the concentration where the signal-to-noise ratio was low enough so that the spectrum of the biological agent was barely higher than the noise.

# **Selection of Bioindicators for Non-Contact Monitoring of Decontamination with VHP**

The biological indicators used in this study with H2B-Spectral were the endospores of Geobacillus stearothermophilus (GS) and Bacillus atrophaeus (BA) gram-positive bacteria. GS is commonly used as a bioindicator for sterilization validation studies and periodic check of sterilization cycles [23], whereas BA strains have been extensively used in as indicator for heatand chemical-based decontamination regimens. Contributing factors for both bacterial species are thick protective cell walls, embedded DNA in large amounts (~10% of spore content) of dipicolinic acid, endospores coat architecture with a multilayered structure [24]. While outer layers prevent larger external molecules to enter the spore, the inner layer blocks hydrogen peroxide molecules. The inner layer is also the one that the spore uses to rebuild the bacterial coat after germination. According to [25], treatment with oxidizing agents damages the inner membrane and sensitizes the spores to the subsequent stress that prevents germination of bacterial endospores after exposing them to hydrogen peroxide gas.

The droplets of  $\sim 10^8$  CFU/ml liquid solutions were dried providing  $10^6$  CFU/cm<sup>2</sup> surface concentrations on the sample disks of stainless steel, which were introduced inside the

fluorometer during VHP decontamination procedures. In this study, the LIF intensity was measured mainly using the tryptophan-like spectral channel.

#### **Monitoring Decontamination Kinetics**

For testing the applicability of the LIF method to the RTDM procedure during and after surface decontamination, bleach and VHP were used as decontaminants. A 0.5 % sodium hypochlorite (bleach) solution was freshly prepared by diluting an anhydrous sodium dichloroisocyanurate (NaDCC) powder (Melspring International b.v., The Netherlands) in water before the measurement. The suspension containing the biological contaminant was spread on the copper surface and mixed with 10 ml of 0.5% chlorine solution. The dynamic of decontamination process was then monitored by real-time measurement of laser-induced fluorescence generated by microbial compounds. VHP was used at various concentrations, and decontamination was carried out in closed environments of 1 m<sup>3</sup> and 30 m<sup>3</sup>. The VHP at controlled concentrations was generated by VCS-100 device [26]. The concentrations of 100, 200, and 300 ppm were used for RTDM with both (GS and BA) sample disks. Higher concentration of 400ppm was added when using GS spores.

# **Results**

#### **Intrinsic Fluorescence of Surface Materials**

Before carrying out RTDM on contaminated surfaces, the intrinsic fluorescence of each uncontaminated background material was measured and the corresponding LIF spectra were taken as a reference (Figure 4b). All fluorescence spectra using an excitation wavelength of 248 nm covered a spectral range between 380 and 520 nm with main fluorescence bands appearing beyond 400 nm, with the notable exception of the band corresponding to PVC plastic which produced a fluorescence peak at 310 nm. The LIF spectra showed major variations between two extremes: as desired, the copper plate produced no fluorescence signal whereas lab coat and PVC plastic produced the highest peaks, being 100 and 10 times higher than other materials used, respectively. These recorded

LIF spectra constituted the reference data set of spectral backgrounds on which the fluorescence of the contaminated surfaces should be analysed.

# Spectral Analysis of Microbial Contaminants on Solid Surfaces

The LIF spectra of each component of the microbial solution (i.e., microbial agents, PBS and TBS solutions, and growth media) and clean versus contaminated surfaces have been measured to compile a global data set for building the BC-Sense classifier. The goal was to use the classifier to enable distinguishing the contaminated surfaces from clean or completely decontaminated ones, irrespective of the arbitrary combination of surfaces and microbial contaminants. Due to a limited training dataset, an ensemble learning strategy, namely Bootstrap aggregation [27,28], was applied in order to discriminate among different types of biological contamination and surfaces. Wavelet feature extraction and selection were also used before application of the analysis algorithm, as previously reported [29].

# Microbial Contaminants Fluorescence using Non-Fluorescent Solid Support

The LIF spectra of microbial contaminants were measured with the samples placed on the copper plate. As no fluorescence is generated by copper (see supra: Intrinsic fluorescence of surface materials), each spectrum was considered to exclusively result from the microbial contaminant solution. The LIF data recorded with various microbial samples revealed similarities and differences (Figure 5). With an excitation wavelength of 248 nm, bacterial models produced a maximal fluorescence intensity at 330 nm, attributed to tryptophan [7]. The spectra characterizing Bacillus spores, C. herbarum conidia, and MS2 bacteriophage differed markedly from bacterial spectra. The fluorescence maxima were observed at 410, 360 and 430 nm. respectively, and are therefore easily distinguishable. At the excitation wavelength of 248 nm, dead and living E. coli bacteria had a similar LIF spectral shape. The fluorescence spectrum of dead E. coli exhibited a shoulder near 450 nm and a higher

fluorescence intensity compared to living *E. coli* and *B. thuringiensis* (Figure 6).

At the excitation wavelength of 351 nm, the LIF spectrum of dead *E. coli* contained noticeable fluorescence in the spectral range of 400-500 nm, not seen with living counterparts attributed to NADH (Figure 6) [30,31].

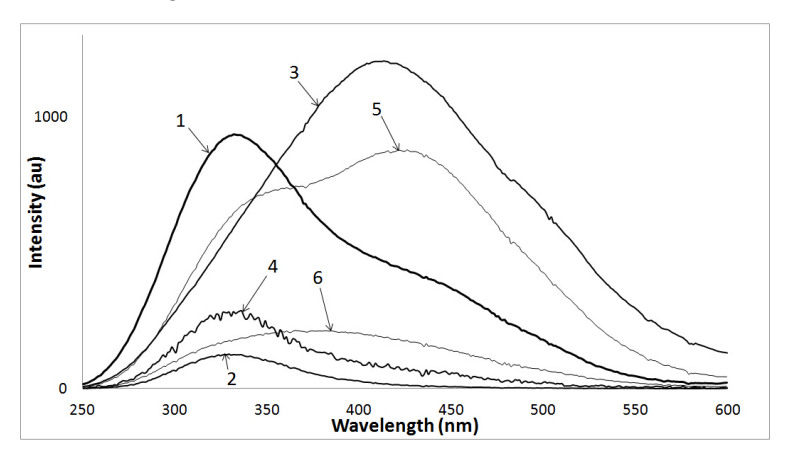


**Figure 5:** LIF spectra of biological contaminants at the excitation wavelength of 248nm. *E. coli* (dead bacteria) 6×10<sup>10</sup> CFU/ml (1), *E. coli* (living bacteria) 1×10<sup>7</sup> CFU/ml (2), *Bacillus* spores 5 g/ml (3), *B. thuringiensis* 2×10<sup>8</sup> CFU/ml (signal multiplied by 10 for visibility) (4), MS2 Virus 1×10<sup>9</sup> PFU/ml (5), *Cladosporium herbarum* (unknown concentration) (6)

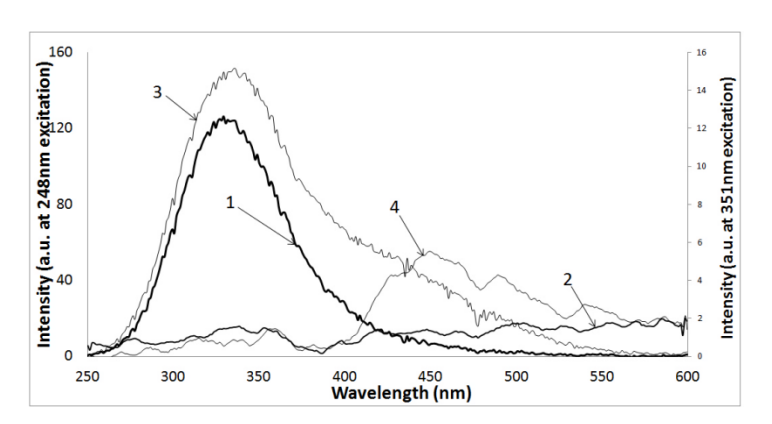


**Figure 6:** LIF spectra of living and dead bacteria E. coli. 1 – living *E. coli* excited at 248 nm, 2 – living *E. coli* excited at 351 nm, 3 – dead *E. coli* excited at 248 nm, 4 – dead *E. coli* excited at 351 nm

LoD calculated using LIF calibration curves for E. coli bacteria and the MS2 virus were 2.9 x10<sup>4</sup> and 9.5 x 10<sup>4</sup> CFU/cm<sup>2</sup>, respectively. The LoQ values were 3.4 x 10<sup>5</sup> and 10<sup>6</sup> PFU/cm<sup>2</sup> for living *E. coli* and MS2 bacteriophage virus, respectively (Table 1).

Table 1: Limits of Detection (LoD) and Quantification (LoQ) of the experimental setup

Biological	LoD	LoQ	RSD	R <sup>2</sup>	Linearity	Range	Recovery	Units
agent			(%)				(%)	/ cm <sup>2</sup>
E. coli	$2.85^4$	$9.49^4$	6.21	0.99	8 <sup>4</sup> - 8 <sup>5</sup>	9 <sup>4</sup> - 8 <sup>5</sup>	103.00	CFU
(alive)								
MS2 virus	$3.36^{5}$	$1.12^{6}$	10.97	0.97	4 <sup>5</sup> - 4 <sup>6</sup>	$1^6 - 4^6$	99.00	PFU

# Spectral Analysis of Microbial Contaminants on Solid Surfaces

The total set of LIF spectra collected during the experiment consisted of more than 800 samples measured in replicates. The training dataset for the classifier consisted of 101 spectra of *E. coli* and MS2 contaminants and a panel set of microbial-uncontaminated solid surfaces (n=85) with their respective fluorescence. The training dataset "out-of-bag" error was 0.08. The LIF spectra of bacterial spores and fungal conidia were not included in the training dataset but used in the test data set. The test dataset consisted of 628 samples, with 37 false and 47 unknown results.

The classifier was created as detailed above (see spectral analysis of microbial contaminated solution on solid surfaces) and embedded into the RTDM procedure of the BC-Sense device. When a LIF spectrum was recorded by the BC-Sense, the classifier instantly produced the value of predicted response (PR) ranging from 0 (lack of contamination) to 1 (100 % probability of contamination).

Random samples (n=200) were assessed. For the clarity of the resulting visualization, the PR of the classifier was distributed in four different groups based on LIF spectra (Figure 7). Group I presented the data recorded with a panel of uncontaminated

surface materials: PR was consistently < 0.25, according to the classifier. Group II included *E. coli* on various surfaces versus solvents: PR was > 0.6 and < 0.3, respectively. Group III presented the LIF data recorded with MS2 virus on various surfaces versus culture media used for bacterial and viral growth: PR was > 0.6 and < 0.2, respectively. Group IV included the LIF spectra generated by bleach alone versus bacterial spores and fungal conidia-contaminated solid surfaces. In this group, the classifier discriminated contaminated surfaces (PR > 0.6) from bleach (PR < 0.2).

Data analysis concerning PR showed that two thresholds discriminate between contamination and background signals: < 0.4 considered as negative whereas > 0.55 being considered contaminated. As expected, the classifier was not able to detect contamination when surface contamination was carried out with a microbial concentration near the LoD of the BC-Sense tool (Table 1). The spectral shape and intensity of fluorescence of background surfaces influenced the detection capability. In particular, E. coli was correctly detected by the classifier on PVC, canvas tent, and aluminium, while its detection on Plexiglas/PMMA and galvanized steel was challenging. In the latter case, the detection reliability depended indeed on the bacterial concentration. The MS2 virus was successfully detected on Plexiglas/PMMA, canvas tent, PVC, aluminium and steel. As described above uncontaminated background materials, solvents and growth media were always correctly discriminated by the classifier (Figure 7).

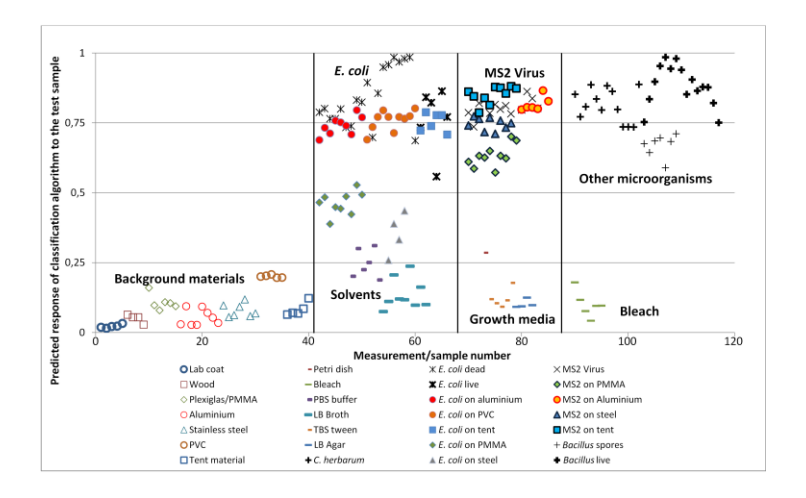


**Figure 7**: Analysis result for different classes of spectra. BC-sense analysis of solvents, growth media, and solid surfaces with and without microbial contaminants: data mining and result analysis. The predicted response (PR) of the BC-sense classifier for 200 random samples of solvents, growth media, and solid surfaces with and without microbial contaminants: group I – PR < 0.25 for clean surfaces; group II – PR < 0.3 for solvents and PR < 0.6 for the surfaces contaminated by E. coli; group III – PR <0.2 for media samples and PR > 0.6 for the surfaces contaminated by MS2 virus; group IV – PR < 0.2 for the bleach and PR > 0.6 for bacterial spores and fungal conidia. Blank markers and thin noughts below 0.45 PR represent pure background materials, nutrient solutions and blank, felled markers and bold noughts above 0.55 PR represent cultures of microorganisms and materials contaminated by them.

# **Online RTDM during the Decontamination Process**

BC-Sense LIDAR device was finally used to monitor in real-time the kinetics of decontamination when treating contaminated surfaces by bleach. The decontamination efficiency expressed as a decrease in fluorescence intensity was assessed on surfaces contaminated with living *E. coli* cells, MS2 bacteriophage and spores of *B. thuringiensis*. The dynamic decrease in fluorescence intensity was monitored in real-time on the corresponding LIF spectra. Pouring 0.5 % chlorine solution directly onto a microbial-contaminated surface generated indeed an immediate and abrupt drop of fluorescence. With MS2, complete disappearance of the fluorescence was achieved in 1 minute whereas this lasted longer (up to 10 min) with *E. coli* and spores of *B. thuringiensis* (Figure 8).

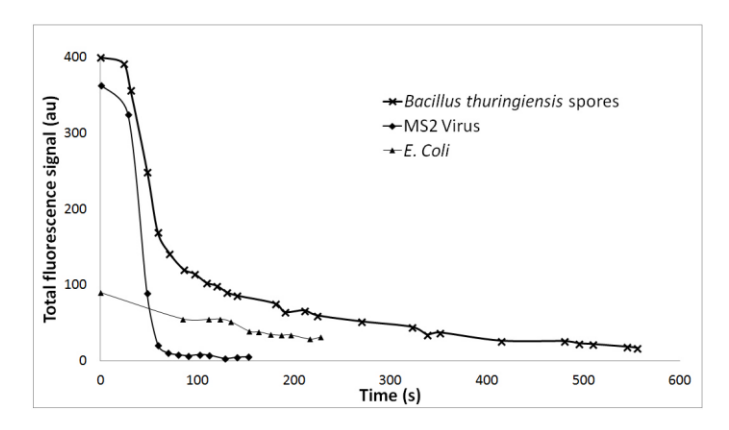


**Figure 8:** Bleach decontamination kinetics. Decrease of the integral fluorescence signal, in the spectral range 250 nm to 600 nm, during microbial decontamination of *Bacillus* spores, MS2 bacteriophages and *E. coli* due to surface decontamination with 0.5 % sodium hypochlorite solution

The experiments with VHP were initially carried out inside a specially designed experimental chamber of 1 m<sup>3</sup> volume. The experiments revealed a clear drop in the fluorescence intensity of the sample disk with BA spores under VHP treatment. The decrease was observed as soon as the VHP generator VCS-100 was switched on. The decrease in fluorescence intensity at 340nm (tryptophan-like fluorescence) persisted, which can be attributed to permanent oxidative damage of the spores (Figure 9). In line with previous hypotheses on tryptophan fluorescence quenching by hydrogen peroxide [14], additional experiments were conducted using pure L-Tryptophan (Sigma-Aldrich) under the same experimental conditions as with BA spores. The surface concentration of L-Tryptophan on the sample disk was around 5 µg/cm2 to match the initial fluorescence intensity produced by BA spores. Compared to pure tryptophan, the fluorescence intensity of BA-bound tryptophan dropped much faster (Figure 9). This indicates that the decrease in the tryptophan fluorescence generated by BA spores likely reflects the impact hydrogen peroxide on living cells, most probably due to changes in the bacterial cell structure, functioning, and viability.

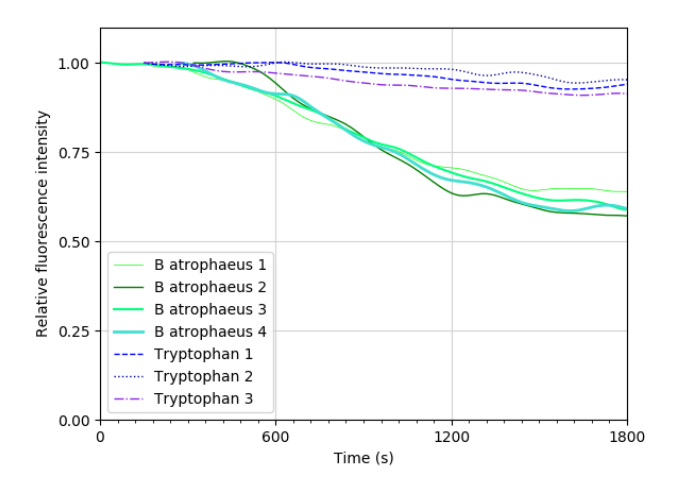
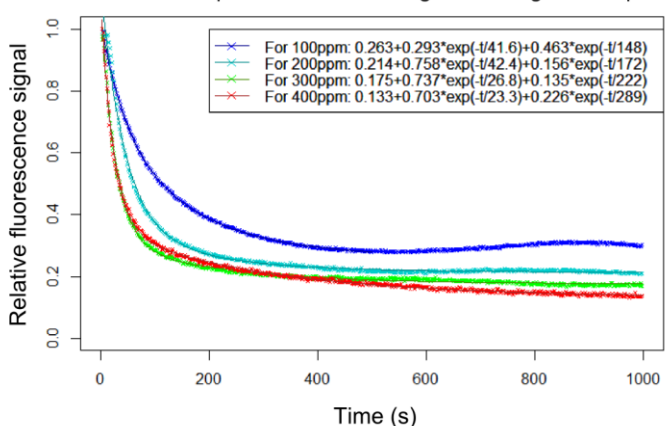


**Figure 9:** Fluorescence signal fall-off in pure L-Tryptophan versus *B. atrophaeus* spores under equal low concentration (100-200ppm) VHP treatment

To establish the repeatability of the decontamination monitoring extensive experiments were conducted experimental chamber and closed room. During successive experiments at fixed conditions of surface concentration of spores (~10<sup>6</sup> CFU/cm<sup>2</sup>), VHP concentration and treatment duration. The process monitoring was highly repeatable, and the fluorescence fall-off rate was highly correlated with VHP concentrations with a low threshold of ~300 ppm (Figure 10). A higher VHP concentration caused faster fluorescence fall-off rate, followed by a plateau phase at completion of the decontamination. The experimental data show that the plateau to which the spectral intensity decreases is also concentration dependent. A higher VHP concentration leads to a lower relative fluorescence level at the end of exposure as expected from fluorescence quenching effects and oxidation of tryptophan by hydrogen peroxide.



Fit functions for GS spore fluorescence signals during VHP exposure

**Figure 10:** Intensity of relative fluorescence levels in tryptophan-like spectral region as function of time at 100ppm, 200ppm, 300ppm and 400ppm VHP concentrations. Data were acquired in real-time after placing the samples in the experimental room (t=0) where VHP decontamination takes place

#### **Discussion**

Various methods are currently used for the detection of microbiological contamination on surfaces. e.g. ATPbioluminescence assay [30], PCR-based methods [31] and a large variety of optical methods [32]. Most of them, especially nucleic acid- and antibody-based assays, are cumbersome, expensive, and require a longer turnaround time. Before the analytical step, samples need first to be collected from targeted before undergoing adequate processing. bioluminescence assay requires preliminary surface preparation with specific antibodies, hence providing at best questionable results, whereas other assays require rather complex analysis of collected samples.

Global issues related to surface contamination, and detection thereof, were evidenced during the last Ebola outbreak in West Africa. They perfectly illustrate the current technological challenges. During this outbreak, the risk of nosocomial transmission through indirect Ebola virus (EBOV) transmission via surfaces or fomites contaminated with the patient's blood or

body fluids was a daily concern. Whilst the incidence of nosocomial infection within Ebola healthcare facilities remains contentious, several contaminations indeed occurred in health care workers (HCWs) regardless of strict infection prevention and control measures. This outlined the need to improve the understanding of the EBOV environmental transmission, i.e. how long and where does the virus survive in real-life conditions and whether it withstands current decontamination protocols. Accordingly, surface swabbing followed by EBOV-specific RNA-based assay was proposed to assess viral persistence in the immediate vicinity of Ebola patients, namely on the material in contact with patients like beds, mattresses, and linens, as well as on HCWs personal protective equipment and gloves [33-37]. Results demonstrated the relatively high stability of viral RNA, especially in high temperatures and moist conditions, as is the case in tropical settings. In addition to this, there was mounting evidence that EBOV can remain viable on surfaces for several days under simulated environmental conditions for the climate of West Africa [38]. Altogether, these results advocated the detection of EBOV RNA as a surrogate marker of viral contamination of the environment and its use as the most sensitive measure of safety. Nucleic acid-based assay appeared to be the best and only method for residual hazard assessment, i.e. complete versus incomplete decontamination according to whether RNA disappears or not. Nevertheless, due to biosafety and regulatory issues, none of the above studies could carry out viral culture in the field, in real operational conditions, nor could samples be exported abroad for confirmatory testing [34,36,37]. Consequently, genuine study limitations such as lack of confirmation of the viability and infectivity of EBOV from RNA-positive specimens tempered the interpretation of RNAbased results. Moreover, it should not be overlooked that EBOV culture can produce false-negative results with the swabbing method, especially when the microbial load is low, hence making questionable the reliability of a negative viral culture from RNA EBOV positive samples [33,39].

Interestingly enough, constraints and issues associated with potential microbial surface contamination extend far beyond the Ebola case. Indeed, swabs and wipes followed by sample processing have long been applied in different fields among which medical applications [40,41], food safety [42-44], and biothreat assessment [45,46]. However, a series of limitations strongly affect this type of safety control protocol among which a size-biased sampling, the type of sampling field, the nature of environmental swab samples which makes the use of multiple swabs on the same site impossible, and the use of the different collection and analytical methods limiting their applicability to the real-world setting. Consequently, sampling inconsistency cannot be ruled out and technique variability in sample collection may be responsible for discordant results. Besides, swabbing does not always lend itself to use with life-threatening agents owing to biosafety concerns during processing.

Therefore, evidence-based decontamination procedures should protect those at risk of contamination from environmental sources (hospitalized patients, hospital staff, population...) or from the intentional release of biological agents using fieldbased tools that can serve as surrogate measures of viable or dead microbial agents on surfaces, without neither sampling nor acid nucleic-based analysis. So far, only scarce data report on methods that allow RTDM of microbial contaminants, mainly for medical [47] or food applications [48,49]. The LIF method dual-wavelength sensing and multispectral pattern recognition enables BC-Sense LIDAR for stand-off detection based on the primary component analysis of intrinsic fluorescence spectra of biological models [4]. According to current results, spectral shapes allowed distinguishing between groups of biological agents and background (e.g. culture medium, solvents and surface material) while minimizing falsepositive results [29]. A panel of microbial agents on a range of solid surfaces were correctly classified without sample collection nor analytical procedure and with a turnaround time < 3 seconds for each identification test. Consistent discrimination of contaminated versus non-contaminated surfaces was possible using optimal thresholds as defined here, i.e., PR > 0.55 as indicator of surface contamination and PR < 0.4 for surface cleanliness. Provisional identification of the group of biological agent was obtained by using a robust decision tree-learning algorithm that compared the fluorescence spectra of unknown

microbial contaminants with a database of > 800 samples collected during this study.

The fluorescence maximum peak of bacteria excited at 248 nm is attributable to tryptophan fluorescence. The fluorescence spectra of dead and living E. coli looked comparable except at 351 nm excitation where the difference was supposedly related to NADH fluorescence. In some studies, NADH fluorescence is indeed used as biomarker of cell viability [10,50] and/or cell death [51]. NADH expression increases after induction of cell injury or death and decreases until cell death [52], making it an interesting marker to discriminate between alive and dead bacterial cells. In line with previous reports [53], bacillus spores, MS2 bacteriophage and C. herbarum conidia showed different spectra compared with bacteria, which make them easily recognizable. The fluorescence of bacteriophage MS2 is attributed to the tyrosine in the coat protein [54,55]. While the most efficient spectral range to excite the fluorescence of tyrosine is 275-300 nm, the sensing wavelength 248 nm of BC-Sense induced its noticeable fluorescence as well. Viral LIF spectra showed two peaks, the highest being around 430 nm, suggesting that this part of the spectra may be influenced by E. coli lysate (dead cells) following viral replication [53]. Anyhow, the viral spectrum differs from both alive and dead bacteria spectra, outlining the ability of BC-Sense to identify the type of biological contamination. It is also noteworthy that current detection and quantification limits, evaluated with live E. coli and MS2, are relatively high and should be improved. Nevertheless, the results are promising. Further technological developments combined with database enrichment with fluorescence spectra from additional biological models and the background material will undoubtedly improve the limit of detection and quantification.

Regarding surface decontamination, the most common cleaning fluid used is a chlorine solution (bleach). The primary decontamination effect occurs because hypochlorite anions oxidize and denature the large three-dimensional structure of proteins, opening them up and altering the amino acids which lie inside [56]. The chlorine solution destroys the biomolecules in time scale from seconds to minutes depending on the type of

microorganisms. The BC-Sense tool enabled operators to follow in real-time the decontamination kinetics of the chlorine treatment using biological models with varying bleach sensitivity (e.g virus more sensitive than spores). The monitoring of cleaning efficiency, using different decontamination solutions on an extensive panel of biological agents (e.g. spores, viruses, bacteria, and toxins) and surfaces (porous versus non-porous material), will help optimize decontamination protocols and methods. This is also very much needed, knowing that bleach may cause serious damage to equipment used in a contaminated environment [22].

The H2B-Spectral device usefully complements the medium-range stand-off RTDM. It can indeed be rapidly used to monitor the decontamination process after pathogens have been detected by BC-Sense and afterwards as a control of the quality of the decontamination process. The quenching effects of VHP on fluorescent protein residues reflect indeed VHP decontamination efficiency, hence being a useful indicator of decontamination quality and completeness. Alternatively, H2B-Spectral can also be used point detector in biowarfare agent applications, as first tested during the international Bio-Garden CBRN exercise organized in the framework of the European Commission H2020 project eNOTICE (European Network of CBRN Training Centres) [12,13,57] (Figure 11). This technology appears also very useful for the risk assessment of uncontrolled or accidental contamination in a mobile laboratory [58-60].



**Figure 11:** First use of the H2B Spectral prototype sensor in the framework of the Bio-Garden exercise. The left panel and right panels the use of H2B prototype to test the presence of biological agents on the door of the mimicked clandestine laboratory with by a military first-responder from the intervention squad (a), and the same military first-responder at work (b). This international exercise focused on rapid detection of biological agents in a clandestine laboratory. Held on 19 June 2018 at the Belgian Defence barracks Major Housiau, Vilvoorde (Peutie), Belgium, Bio-Garden was organized jointly by the H2020 project eNOTICE, UCL/CTMA team, and the ESA B-LIFE telecommunication consortium.

### **Conclusions**

In conclusion, the developed BC-Sense device and H2B-Spectral sensor proved that the LIF method enables a user-friendly RTDM of microbial contamination/decontamination on solid surfaces. Such stand-off or non-contact application of RTDM has a high positive impact in terms of biosafety as it provides first responders with a better situational awareness without the manipulation and transport of potentially dangerous samples, hence limiting personal exposure to biological agents and the

risk of spreading the contamination. A quick determination of the extent and nature of suspected microbial contamination using multispectral LIF data without sampling is paramount for risk assessment and decision making on sample collection in the appropriate biosafety conditions (i.e., level of protective equipment and standard operating procedures for sampling and safe packaging). The real-time measurement of tryptophan fluorescence quenching during VHP treatment can be used as a reliable online technique to control the efficiency of decontamination. LIF data comparison with the live status of micro-organisms, i.e. their growth ability, confirmed that the autofluorescence signal reached a persistent minimal level and therefore reliable and useful evidence provides decontamination completeness. These tools, therefore, fill a major gap in real-time assessment of biological hazards in work environment, residual hazard assessment after decontamination (i.e. decontamination efficiency), and guidance for the type and thoroughness of cleaning procedures.

#### References

- 1. Piette AS, Vybornova O, Bentahir M, Gala JL. CBRN: detection and identification innovations. Crisis Response Journal. 2014; 10: 36-38.
- 2. JM. How clean is clean enough? CBRNe WORLD. 2009; Autumn. 2009; 68-70.
- Hausmann A, Duschek F, Fischbach T, Pargmann C, Aleksejev V, et al. Standoff detection: classification of biological aerosols using laser induced fluorescence (LIF) technique. InChemical, Biological, Radiological, Nuclear, and Explosives (CBRNE) Sensing International Society for Optics and Photonics. 2014; 9073: 90730Z.
- 4. Sohn M, Himmelsbach DS, Barton FE, Fedorka-Cray PJ. Fluorescence spectroscopy for rapid detection and classification of bacterial pathogens. Applied spectroscopy. 2009; 63: 1251-1255.
- Sedlacek AJ, Ray MD, Higdon NS, Richter DA, editors. Short-range noncontact detection of surface contamination using Raman lidar. Vibrational Spectroscopy-based Sensor

- Systems. International Society for Optics and Photonics. 2002; 4577: 95-104.
- Multari RA, Cremers DA, Dupre JAM, Gustafson JE. Detection of biological contaminants on foods and food surfaces using laser-induced breakdown spectroscopy (LIBS). Journal of agricultural and food chemistry. 2013; 61: 8687-8694.
- 7. Tao F, Peng Y, Li Y, Chao K, Dhakal S. Simultaneous determination of tenderness and Escherichia coli contamination of pork using hyperspectral scattering technique. Meat Science. 2012; 90: 851-857.
- 8. Ghisaidoobe AB, Chung SJ. Intrinsic tryptophan fluorescence in the detection and analysis of proteins: a focus on Förster resonance energy transfer techniques. International journal of molecular sciences. 2014; 15: 22518-22538.
- 9. Nevin A, Cather S, Anglos D, Fotakis C. Analysis of protein-based binding media found in paintings using laser induced fluorescence spectroscopy. Analytica chimica acta. 2006; 573: 341-346.
- 10. Liang J, Wu WL, Liu ZH, Mei YJ, Cai RX, et al. Study the oxidative injury of yeast cells by NADH autofluorescence. Spectrochimica Acta Part A: Molecular and Biomolecular Spectroscopy. 2007; 67: 355-359.
- 11. Nyabi O, Bentahir M, Ambroise J, Bearzatto B, Chibani N, et al. Diagnostic Value of IgM and IgG Detection in COVID-19 Diagnosis by the Mobile Laboratory B-LiFE: A Massive Testing Strategy in the Piedmont Region. International Journal of Environmental Research and Public Health. 2021; 18: 3372.
- 12. Nyabi O, Vybornova O, Gala JL. Deployment of a Mobile Laboratory for the Control and Monitoring of High-Consequence Infectious Diseases: An Illustration With the Ebola Virus, the Biowarfare Agents, and the COVID-19. Journal of Strategic Innovation & Sustainability. 2021; 16.
- 13. Vybornov A, Nyabi O, Vybornova O, Gala JL. Telecommunication Facilities, Key Support for Data Management and Data Sharing by a Biological Mobile Laboratory Deployed to Counter Emerging Biological Threats and Improve Public Health Crisis Preparedness.

- International Journal of Environmental Research and Public Health. 2021; 18: 9014.
- 14. Cooper GM, Hausman RE. The cell: Sinauer Associates Sunderland; 2000.15. Harwood CR. Bacillus subtilis as a Model for Bacterial Systems Biology. eLS. 2007.
- 15. Greenberg DL, Busch JD, Keim P, Wagner DM. Identifying experimental surrogates for Bacillus anthracis spores: a review. Investigative genetics. 2010; 1: 4.
- 16. Schubert K, Groenewald J, Braun U, Dijksterhuis J, Starink M, et al. Biodiversity in the Cladosporium herbarum complex (Davidiellaceae, Capnodiales), with standardisation of methods for Cladosporium taxonomy and diagnostics. Studies in Mycology. 2007; 58: 105-156.
- 17. O'Connell KP, Bucher JR, Anderson PE, Cao CJ, Khan AS, et al. Real-time fluorogenic reverse transcription-PCR assays for detection of bacteriophage MS2. Applied and environmental microbiology. 2006; 72: 478-483.
- 18. Bentahir M, Laduron F, Irenge L, Ambroise J, Gala JL. Rapid and Efficient Filtration-Based Procedure for Separation and Safe Analysis of CBRN Mixed Samples. PloS one. 2014; 9: e88055.
- Kropinski AM, Mazzocco A, Waddell TE, Lingohr E, Johnson RP. Enumeration of bacteriophages by double agar overlay plaque assay. Bacteriophages: Methods and Protocols, Volume 1: Isolation, Characterization, and Interactions. 2009; 69-76.
- 20. Armbruster DA, Pry T. Limit of blank, limit of detection and limit of quantitation. The Clinical Biochemist Reviews. 2008; 29: S49-S52.
- 21. Irenge LM, Dindart JM, Gala JL. Biochemical testing in a laboratory tent and semi-intensive care of Ebola patients onsite in a remote part of Guinea: a paradigm shift based on a bleach-sensitive point-of-care device. Clinical Chemistry and Laboratory Medicine. 2017; 55: 1881-1890.
- 22. Luftman HS, Regits MA, B Atrophaeus. Stearothermophilus Biological Indicators for Chlorine Dioxide Gas Decontamination. Applied Biosafety. 2008; 13: 143-157.
- 23. McKenney P, Driks A, Eichenberger P. The Bacillus subtilis endospore: assembly and functions of the multilayered coat. Nat Rev Microbiol. 2013; 11: 33–44.

- 24. Cortezzo D, Koziol-Dube K, Setlow B, Setlow P. Treatment with oxidizing agents damages the inner membrane of spores of Bacillus subtilis and sensitizes spores to subsequent stress. Journal of Applied Microbiology. 2004; 97: 838-852.
- 25. VCS-100 HPV device description. Available online at: https://cleamix.com/products/
- 26. Breiman L. Bagging predictors. Machine learning. 1996; 24: 123-140.
- 27. Breiman L. Random forests. Machine learning. 2001; 45: 5-32.
- 28. Sobolev I, Babichenko S. Application of the wavelet transform for feature extraction in the analysis of hyperspectral laser-induced fluorescence data. International journal of remote sensing. 2013; 34: 7218-7235.
- 29. Aiken ZA, Wilson M, Pratten J. Evaluation of ATP bioluminescence assays for potential use in a hospital setting. Infection Control & Hospital Epidemiology. 2011; 32: 507-509.
- 30. Talkington DF. PCR Detection of Microbial Pathogens. Emerging infectious diseases. 2013; 19: 1353.
- 31. Fischer M, Triggs G, Krauss TF. Optical sensing of microbial life on surfaces. Applied and environmental microbiology. 2016; 82: 1362-1371.
- 32. Bausch DG, Towner JS, Dowell SF, Kaducu F, Lukwiya M, et al. Assessment of the risk of Ebola virus transmission from bodily fluids and fomites. The Journal of infectious diseases, 2007; 196: S142-S147.
- 33. Youkee D, Brown CS, Lilburn P, Shetty N, Brooks T, et al. Assessment of environmental contamination and environmental decontamination practices within an ebola holding unit, Freetown, Sierra Leone. PloS one. 2015; 10: e0145167.
- 34. Cook BW, Cutts TA, Nikiforuk AM, Poliquin PG, Strong JE, et al. Evaluating environmental persistence and disinfection of the Ebola virus Makona variant. Viruses. 2015; 7: 1975-1986.
- 35. Poliquin PG, Vogt F, Kasztura M, Leung A, Deschambault Y, et al. Environmental contamination and persistence of Ebola virus RNA in an Ebola treatment center. The Journal of infectious diseases. 2016; 214: S145-S152.

- 36. Palich R, Irenge LM, de Sainte Fare EB, Augier A, Malvy D, et al. Ebola virus RNA detection on fomites in close proximity to confirmed Ebola patients; N'Zerekore, Guinea, 2015. PloS one. 2017; 12: e0177350.
- 37. Fischer R, Judson S, Miazgowicz K, Bushmaker T, Prescott J, et al. Ebola virus stability on surfaces and in fluids in simulated outbreak environments. Emerging infectious diseases. 2015; 21: 1243.
- 38. Spengler JR, McElroy AK, Harmon JR, Ströher U, Nichol ST, et al. Relationship between Ebola virus real-time quantitative polymerase chain reaction—based threshold cycle value and virus isolation from human plasma. The Journal of infectious diseases. 2015; 212: S346-S9.
- Kovach CR, Taneli Y, Neiman T, Dyer EM, Arzaga AJA, et al. Evaluation of an ultraviolet room disinfection protocol to decrease nursing home microbial burden, infection and hospitalization rates. BMC infectious diseases. 2017; 17: 1-8
- 40. Varona-Barquin A, Ballesteros-Peña S, Lorrio-Palomino S, Ezpeleta G, Zamanillo V, et al. Detection and characterization of surface microbial contamination in emergency ambulances. American journal of infection control. 2017; 45: 69-71.
- 41. Rönnqvist M, Rättö M, Tuominen P, Salo S, Maunula L. Swabs as a tool for monitoring the presence of norovirus on environmental surfaces in the food industry. Journal of food protection. 2013; 76: 1421-1428.
- 42. Patel D, Stansell J, Jaimes M, Ferris K, Webb G. A Survey of Microbial Contamination on Restaurant Nonfood-Contact Surfaces. Journal of Food Safety. 2017; 37: e12287...
- 43. Keeratipibul S, Laovittayanurak T, Pornruangsarp O, Chaturongkasumrit Y, Takahashi H, et al. Effect of swabbing techniques on the efficiency of bacterial recovery from food contact surfaces. Food Control. 2017; 77: 139-144.
- 44. Locascio LE, Harper B, Robinson M, Badar T. Standard practice for bulk sample collection and swab sample collection of visible powders suspected of being biological agents from nonporous surfaces: collaborative study. Journal of AOAC International. 2007; 90: 299-333.

- 45. Pazienza M, Britti M, Carestia M, Cenciarelli O, D'Amico F, et al. Application of real-time PCR to identify residual biodecontamination of confined environments after hydrogen peroxide vapor treatment: preliminary results. J Microb Biochem Technol. 2013; 6: 24-28.
- 46. Hassan M, Gonzalez E, Hitchins V, Ilev I. Detecting bacteria contamination on medical device surfaces using an integrated fiber-optic mid-infrared spectroscopy sensing method. Sensors and Actuators B: Chemical. 2016; 231: 646-654
- 47. Everard CD, Kim MS, Lee H. Assessment of a handheld fluorescence imaging device as an aid for detection of food residues on processing surfaces. Food Control. 2016; 59: 243-249.
- 48. Vejarano R, Siche R, Tesfaye W. Evaluation of biological contaminants in foods by hyperspectral imaging (HSI): A review. Int. J. Food Prop. 2017; 20: 1264-1297.
- 49. Luger-Hamer M, Barbiro-Michaely E, Sonn J, Mayevsky A. Renal viability evaluated by the multiprobe assembly: a unique tool for the assessment of renal ischemic injury. Nephron Clinical Practice. 2009; 111: c29-c38.
- 50. Buschke DG, Squirrell JM, Fong JJ, Eliceiri KW, Ogle BM. Cell death, non-invasively assessed by intrinsic fluorescence intensity of NADH, is a predictive indicator of functional differentiation of embryonic stem cells. Biology of the Cell. 2012; 104: 352-364.
- 51. Wang HW, Wei YH, Guo HW. Reduced nicotinamide adenine dinucleotide (NADH) fluorescence for the detection of cell death. Anti-Cancer Agents in Medicinal Chemistry (Formerly Current Medicinal Chemistry-Anti-Cancer Agents). 2009; 9: 1012-1017.
- 52. Pan YL. Detection and characterization of biological and other organic-carbon aerosol particles in atmosphere using fluorescence. Journal of Quantitative Spectroscopy and Radiative Transfer. 2015; 150: 12-35.
- 53. Fraser D, Jerrel EA. The amino acid composition of T3 bacteriophage. Journal of Biological Chemistry. 1953; 205: 291-295.

- 54. Hooker JM, Kovacs EW, Francis MB. Interior surface modification of bacteriophage MS2. Journal of the American Chemical Society. 2004; 126: 3718-3719.
- 55. Ledford H. How does bleach bleach? Nature. 2008.
- 56. Bio-Garden Exercise: CCN#2—Proof-of-Concept—Utilisation Plan, CCN#2\_PoC UP, 2018-12-27. IAP—ARTES 20, ESTEC Contract Number: 4000112330/14/NL/US CCN#2. Available online at: https://cdn.uclouvain.be/groups/cms-editors-ctma/dossier-ja/20181227\_B-LiFE-DEMO\_Phase\_CCN\_2\_WP3\_PoC-UP.pdf
- 57. Vybornova O, Vybornova O, Gala JL, Gala JL. Decision support in a fieldable laboratory management during an epidemic outbreak of disease. Journal of Humanitarian Logistics and Supply Chain Management. 2016; 6: 264-295
- 58. Vybornova O, Gala JL. Structured decision-making for the management of a biological fieldable laboratory during outbreaks: a case for European Union Civil Protection Mechanism (EUCPM). Environment Systems and Decisions. 2019; 39: 65-76.
- 59. Vybornova O, Gala JL. Operations management and decision making in deployment of an on-site biological analytical capacity. In Gary P. Moynihan (Ed.) /Contemporary issues and Research in Operations Management, IntechOpen. Chapter. 2018; 4: 53-80.